

Article

Performance Analysis of Axial-Flux Induction Motor with Skewed Rotor

Fatma Keskin Arabul *, Ibrahim Senol and Yasemin Oner

Department of Electrical Engineering, Yildiz Technical University, 34220 Istanbul, Turkey; senol@yildiz.edu.tr (I.S.); yoner@yildiz.edu.tr (Y.O.)

* Correspondence: fkeskin@yildiz.edu.tr

Received: 27 August 2020; Accepted: 21 September 2020; Published: 23 September 2020



Abstract: In recent years, with developing technology in the field of electrical machines, more efficient and high power density electric motors have been produced. The use of high energy efficiency motors gains importance due to the increase in global energy demand. The main purpose of this study was to design an Axial Flux Induction Motor (AFIM) with the same efficiency class as the Radial Flux Induction Motor (RFIM) in premium efficiency (IE3) class which is used commonly in industrial applications. Various AFIMs are designed with different rotor slot numbers and performance analyses as efficiency and torque ripple changes are investigated. It is known that torque ripple is one of the key parameters in electrical machine design which should be kept as low as possible without decreasing efficiency and torque. Accordingly, AFIMs' rotor slots are skewed considering the stator and rotor slot numbers. The use of a Soft Magnetic Composites (SMC) material in design is also investigated. As a result of the analyses, many premium efficiency classes for AFIMs are obtained. In addition, using SMC material and skewing the rotor slots provides that torque ripples be reduced.

Keywords: axial flux induction motor; finite element analysis; performance evaluation

1. Introduction

Today, more than 40% of the global energy consumption amount is consumed by induction motors and this rate exceeds 70% in the industry [1,2]. Additionally, these motors are key components of many industrial processes, with their reliability, and low cost of maintenance and construction [3,4]. Considering the amount of energy consumed by these motors, it is seen that even a small change in their efficiency will provide significant savings in worldwide energy consumption. The largest energy savings, particularly for medium and small power motors, arise for their higher efficiency classes [5,6]. Accordingly, the use of IE3 class motors has become mandatory due to the laws published in many countries. For instance, IE3 motors have been mandatory since 2011 in the United States and in Turkey, China, and the EU countries in 2015 [7–9]. Nowadays, energy consumption and environmental impacts are reduced with high efficiency motors. Additionally, motor reliability increases sustainable use and demand for investment [10]. In many countries around the world, many programs are encouraged to increase the use of high-efficiency motors. Among these programs, the Efficiency Increasing Project and the Efficient Motor Replacement programs are prominent in the world. Replacing existing low-efficiency motors with high-efficiency motors will result in significant energy savings even if same-sized motors are used [11,12]. Otherwise, if AFIMs are preferred over conventional RFIMs, more efficient and smaller volume motors can be designed [13,14].

With the developing technology, electric motors have a more compact structure and many studies are carried out to increase their efficiency. In many studies, instead of radial flux design of induction motors, axial flux design was found to have a more compact structure and it was concluded that their efficiency and torque density could be increased further [14,15].

AFIMs have the same operating principle as RFIM. However, design of these motors is quite different. The main difference is the magnetic flux direction. In conventional radial flux machines, the flux is in radial direction relative to the machine axis. The magnetic flux produced in AFIMs is in axial direction with respect to the machine axis.

In recent decades, AFIMs have been a popular research topic for researchers. Many studies have been conducted in the literature on AFIM design and control [16–18]. Among these studies, the most notable ones are the design and implementation of different structures. Additionally, many AFIMs have been designed for various applications such as pumps, electric vehicles, wind turbine, etc. [19,20] For instance, in electric vehicles, which are among the popular topics of today, AFIMs have different uses such as wheel-directly coupled, on-wheel, or main motor [21]. In some studies, different materials have been used, such as iron, magneto dielectric, superconductors, etc. [22,23].

In this study, AFIMs are designed to have the same efficiency class as RFIM in IE3 efficiency class used in industry. In addition, the rotor is skewed to minimize the torque ripple. In the literature, only stator slot numbers has been taken into consideration to determine the skew angles for the performance analysis of an induction motor [24–27]. In this study, and different from the literature, skew angles are selected considering both the ratio of stator and rotor slot numbers. Additionally, analyses are carried out using SMC material for stator, rotor, and both stator and rotor of the motor, which provides the best results in terms of efficiency and torque ripple. However, in the analysis results obtained, a considerable decrease in torque ripple over 11% is observed.

Following the introduction, Section 2 presents the topologies of AFMs and design parameters of AFIM. Section 3 introduces model properties, results, and discussion of all various types of AFIM models. Finally, the concluding remarks are presented in Section 4.

2. Methodology

In this section, considering the geometrical properties of the stator/rotor core, radial and axial flux machine equations are presented after the topologies of AFMs are introduced.

2.1. Axial Flux Machine Topologies

A machine with one air gap is the oldest and simplest structure of AFM, has a single-sided motor, and a single stator-single rotor (SSSR). The structure of this machine is easier due to a single air gap [28]. Generally, this machine is the best choice for low torque applications such as fans, pumps, food processors, etc. [29] Also, it can be said that single-sided AFIMs are more resistant to static eccentricity than conventional motors [30,31]. The disadvantage of this type of machine is that bearing life depends on their load. Active material utilization of the SSSR machine is higher [32]. In Figure 1, single-sided AFIM components are shown.

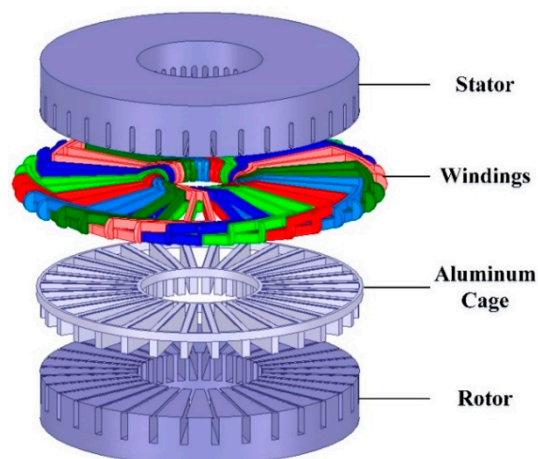


Figure 1. Single-sided Axial Flux Induction Motor (AFIM) components.

There are two air gaps in this type of machine. Both of these air gaps can be axially (double-sided motor), or one axially and the other radially. Such motors consist of a double stator-single rotor, with the rotor sandwiched between the stators, or single stator-double rotor with the stator sandwiched between the rotors. The advantages of double-sided motors include high torque density and balanced axial forces.

In this context, and in terms of economy, the production of two stators is more costly, especially in small powerful machines compared to the single-sided structure. However, the difference in production cost between single-sided motor and double-sided motor for high torque machines is decreasing. In double-sided motors, the moment of inertia is lower and the rotor is lighter [33].

Although the double-sided motor structure has better performance, for high-powered motors, the multi-air-gap disc structure is a better choice [34]. Multi air gap machines have two topologies that are determined by the number of stators and rotors. If the number of stators is more than the number of rotors, these machines are called external stator and internal rotor machines. If the number of rotors is more than the number of stators, these machines are called internal stator external rotor type machines. Internal stator external rotor type machines are preferred due to their high efficiency [35]. This topology can be defined as a concept rather than a machine type. The aim is to place the stators and rotors alternately to meet the requirements of the application. An advantage of this configuration is that it offers modularity [36].

In this study, single air-gap motor topology—which is also prominent in terms of ease of design and analysis—is chosen. It is an advantage that the volume of this structure is smaller. A conventional radial flux induction motor used industrially in the premium efficiency class is taken as a reference to the designed AFIMs.

2.2. Design Parameters of AFIM

The rotating magnetic field can be solved analytically by integrating the basic flux with respect to all radius (r) and pole form factor (α). The rotating magnetic field is within a pole range and electrical angle values are accepted. Axial rotating magnetic field is obtained as in Equation (1).

$$\phi_{ax} = \frac{2B_{max}}{p} (r_2^2 - r_1^2) \cos \omega t \quad (1)$$

where ϕ_{ax} is axial rotating magnetic field in disk-like air gap; B_{max} is maximum induction in the air gap; p is number of poles; r_2 is outer radius of the core of axial induction motor and r_1 is inner radius of the core of axial induction motor.

Basically, the output power of electrical machines (P_2) is a function of flux per pole as in Equation (2).

$$P_2 = f(\phi) \quad (2)$$

Therefore, both types of induction motors can be compared using the flux equations of the rotating magnetic field. In 1986, Varga compared both types of motors using the flux equations of the rotating magnetic field in his study [37]. Thus, the flux equation of AFIM (Equation (1)) has been compared with the similar equation of RFIM (Equation (3)).

$$\phi_{rad} = \frac{4B_{max}}{p} L_r (r_r - r_o) \cos \omega t \quad (3)$$

where ϕ_{rad} is radial rotating magnetic field in cylindrical air gap; L_r is length of the radial induction motor, r_r is rotor radius of the radial induction motor; r_o is radius of shaft opening.

Flux values for two types of motors are equalized for predictive comparison ($\phi_{ax} = \phi_{rad}$), so Equation (4) becomes;

$$2L_r (r_r - r_o) = r_2^2 - r_1^2 \quad (4)$$

In fact, both sides of equation 4 are cross-sectional areas for total magnetic flux in related type induction motors. In Figure 2, RFIM and AFIM geometries are shown. This comparison takes into account only the geometric properties of different types of induction motors under equal magnetic use.

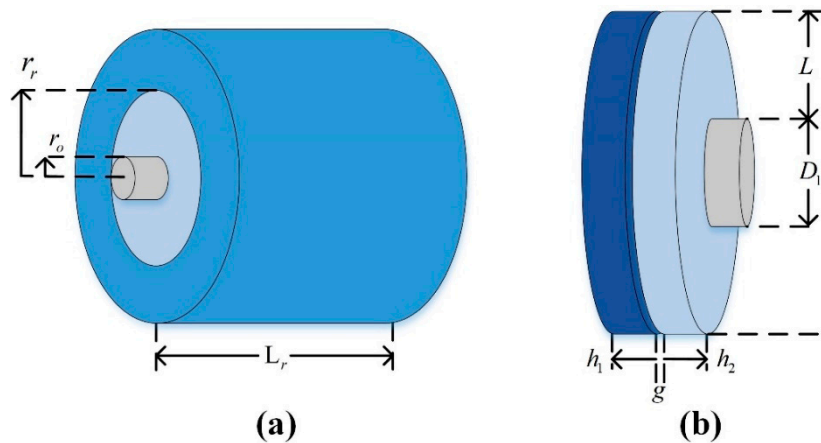


Figure 2. (a) Radial Flux Induction Motor (RFIM) geometry, (b) AFIM geometry.

The shaft opening increases the rotor radius r_r by r_o . The equations given AFIM have a single air gap and no volumetric assumptions are made. In Equation (5), apparent internal power is solved; r_1 and r_2 are halves of D_1 and D_2 , respectively.

$$S_i = C_{ax}(D_2^2 - D_1^2)n_1 \quad (5)$$

where S_i is apparent internal power; C_{ax} is axial induction motor constant; D_2 is core outside diameter with no slots; D_1 is core inside diameter; n_1 is synchronous speed.

In Equation (6), C_{ax} is calculated as;

$$C_{ax} = \frac{\pi^2 \alpha k_w}{\sqrt{2480}} B_{\max} F_1 = \frac{B_{\max} F_1}{109.13} \quad (6)$$

where α is deflection, pole form factor; k_w is winding factor; and F_1 is distributed MMF; k_w and α values are taken 0.9 and 0.7, respectively, as the average values usually used [38].

In Equation (7), D_a refers to the average diameter of the core;

$$D_a = \frac{D_2 + D_1}{2} \quad (7)$$

In Equation (8), L refers to the radial width of the core;

$$L = \frac{D_2 - D_1}{2} \quad (8)$$

While establishing equations for diameter dimensions of AFIM, slots are neglected. The motor air gap is assumed to be constant when the slots are neglected. In these conditions, the outer diameter of the core D_2 can be found as in Equation (9).

$$D_2 = \sqrt{D_1^2 + \frac{2p\phi_{ax}}{B_{\max}}} \quad (9)$$

Core volume of the entire stator and rotor (V) is calculated in Equation (10).

$$V = V_s + V_r = \frac{\pi}{4}(D_2^2 - D_1^2) \sum_i h_i \quad (10)$$

where V_s is core volume of stator; V_r is core volume of rotor; $\sum_i h_i$ is total height of the machine.

Efficiency is calculated as in Equation (11) according to IEEE Standard 112-2017 [39].

$$\eta = \frac{P_{output}}{P_{input}} = \frac{P_{input} - \sum P_{losses}}{P_{input}} \quad (11)$$

where η is efficiency in percent; P_{output} is output power; P_{input} is inner output [39]. $\sum P_{losses}$ is total losses and presented as in Equation (12);

$$\sum P_{losses} = P_{core} + P_{cu} + P_{FW} + P_{STR} \quad (12)$$

where P_{core} is stator and rotor core losses; P_{cu} is stator and rotor copper losses; P_{FW} is mechanical losses as frictional and windage losses and P_{STR} is stray-load losses. The biggest cause of stray-load losses is harmonic energies when the motor is operating under load. If the load current consists of harmonic components, flux magnitude and waveform were distorted, which results in harmonic torques, vibrations and the noise [40,41]. In the IEEE Standard 112-2017, the assumed values for stray-load losses are shown in Table 1. According to the table, in the study, stray-load losses percent of rated load are taken as 1.8% for designed AFIMs [39].

Table 1. Assumed values for stray-load loss.

Machine Rating (kW)	Stray-Load Loss Percent of Rated Load
0.7457 to 90	1.8%
91 to 375	1.5%
376 to 1850	1.2%
1851 and greater	0.9%

In this study, transient analyses are carried out and torque values are calculated with the help of ANSYS Maxwell program. Torque ripple (τ_{ripple}) in percent is defined as the ratio of difference between maximum (τ_{max}) and minimum torque (τ_{min}) values to average torque (τ_{avg}) as in Equation (13).

$$\tau_{ripple} = \frac{\tau_{max} - \tau_{min}}{\tau_{avg}} \cdot 100 \quad (13)$$

AFIM results based on different rotor slot numbers are examined in the next section. In this study, the rotor slots are skewed to achieve better efficiency and fewer torque ripple. Skew angles are given for all slot numbers of the non-skew models, and analyses have been made by taking into account the stator and rotor slot numbers. Skew angle analyses adjusted according to stator slot number are given in Equations (14)–(16).

$$\beta_s = \frac{360}{N_s} \quad (14)$$

$$1.5 \cdot \beta_s = \frac{360}{N_s} = 15^\circ \quad (15)$$

$$2 \cdot \beta_s = \frac{360}{N_s} = 20^\circ \quad (16)$$

where β_s is skew angle according to stator slot number in degrees, N_s is stator slot number. By using Equations (14)–(16); 10° , 15° and 20° are selected. These values are the same for all design and analyzed for all of them.

Skew angle analyses adjusted according to rotor slot number are given in Equations (17) and (18).

$$\beta_r = \frac{360}{N_r} \quad (17)$$

$$2 \cdot \beta_r = \frac{360}{N_r} \quad (18)$$

where β_s is skew angle according to rotor slot number in degrees, N_r is rotor slot number.

In this context, geometries with three additional skew angles, β_s , $1.5 \cdot \beta_s$, $2 \cdot \beta_s$, β_r and $2 \cdot \beta_r$ are applied in the rotor slots of the 28, 30, 32, 34, 38, 40 and 42 slotted models, and analyses results are presented.

3. Results and Discussion

In this section, general design parameters of analyzed AFIMs with reference RFIM are presented. In addition, many AFIMs are designed to be in the same energy efficiency class as the RFIM referenced. While making these designs, no changes are made on the stator. When using the same stator, rotor slot numbers and skew angles are changed.

3.1. RFIM Model Details

This section provides information about the reference RFIM, which is widely used in the industrial applications. The analysis results of this motor, which is IE3 efficiency class with 93.2% efficiency and 7.49% torque ripple, was made by using the ANSYS Maxwell program. Analyses in which the motor model is suitable for 2D analysis are done in two dimensions. The ANSYS model of the model is shown in Figure 3. In addition, general design parameters of RFIM are shown in Table 2.

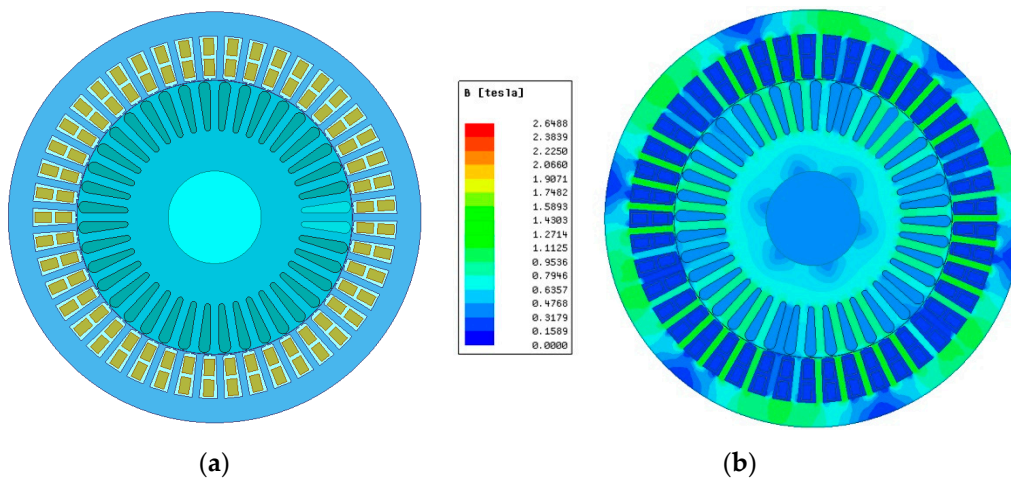


Figure 3. (a) RFIM model (b) Magnetic field density of RFIM.

Table 2. Design parameters of Radial Flux Induction Motor (RFIM).

Parameter	Value
Rated power	30 kW
Rated voltage	400 V
Rated speed	2980 rpm
Rated frequency	150 Hz
Stator core outer diameter	355 mm
Rotor core outer diameter	236.5 mm
Length of motor	250 mm
Stator/Rotor slot numbers	45/40
Stator material	Steel (M19_24G)

3.2. AFIM Model Details

In this section, Finite Element Analysis (FEA) is needed to perform electromagnetic analysis of AFIM. Unlike other types of machines, 3D analysis is mandatory because 2D analysis of such machines does not give detailed results. For this reason, analyses are performed in 3D Cartesian coordinate system and these analyses take a considerable amount of time due to high meshing. Also, for detailed analysis, the number of meshes is kept as high as the processor allowed. In this study, ANSYS Maxwell software is preferred to the FEA analysis, since it is suitable for magnetic field analysis of machines and has a wide usage area.

Firstly, an AFIM designed with the same number of stator and rotor slots. AFIM model and the magnetic field density of AFIM is shown in Figure 4. This model is designed with a non-skewed rotor. According to the analysis results, the efficiency of AFIM is 82.83%, while the torque ripple is 7.4%. Thereafter, in the next section, AFIMs are designed with different rotor slot numbers and various skewed rotors to increase the efficiency to IE3 efficiency class. Table 3 shows the general design parameters of the analyzed AFIMs.

Table 3. General design parameters of Axial Flux Induction Motor (AFIMs).

Parameter	Value
Rated power	30 kW
Rated voltage	400 V
Rated speed	2895 rpm
Rated frequency	150 Hz
Stator/Rotor core outer diameter	355 mm
Stator/Rotor core inner diameter	140 mm
Air-gap length	2 mm
Length of stator/rotor	60/55 mm
Stator slot numbers	36
Rotor slot numbers	28, 30, 32, 34, 38, 40, 42
Stator material	Steel (M19_24G)
Winding type	Whole Coiled
Number of conductors per slot	16
Number of strands	2
Conductor type	Copper

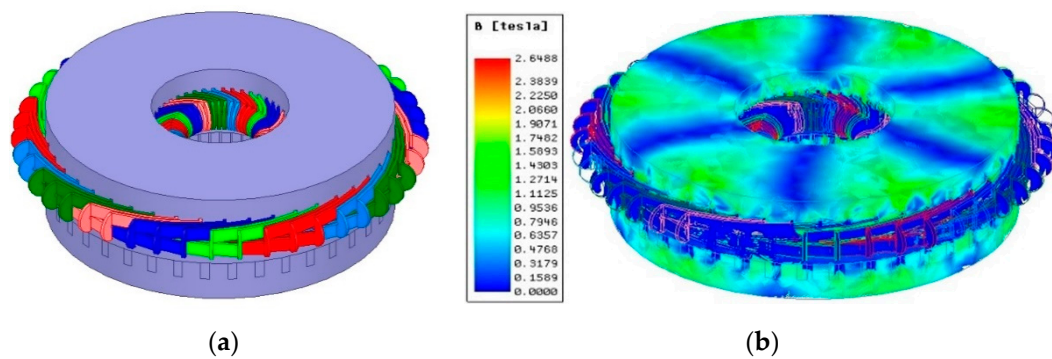


Figure 4. (a) AFIM model (b) Magnetic field density of AFIM.

3.3. AFIM Analyze Results with Different Rotor Slot Numbers

In this section, analyses are made according to seven different slot numbers for the rotor slots without skewing, 28, 30, 32, 34, 38, 40 and 42 slots, respectively. While determining these numbers, rotor slot widths are taken into account according to the machine size. Therefore, the maximum slot number is specified as 42 and the minimum as 28 for the number of rotor slots. Since the stator slot number is 36, 36-slot rotor design is not feasible, and because the stator slot and rotor slot areas are overlapped, the magnetic flux production is not possible.

It is known that torque ripple is one of the most challenging parameters in electrical machine designs. While making designs, decreasing this value is an aim. Therefore, torque ripples are taken into consideration while making comparisons. Figure 5 shows the efficiency and torque ripples of the analysis results according to 7 different slot numbers from 28 to 42. In Figure 5, torque ripple in 30 and 42 slotted AFIMs varies a lot compared to others. As the reason for this, it can be said that the number of these two slots is a multiple of 6; that is, the pole number. Thus, they are forced more in magnetic field transition. From the other five AFIMs, the torque ripples of only 28 and 34 slotted rotor designs are over 10%, while the other three designs' torque ripples at 9%. In this way, AFIM models with the best performance in terms of torque ripples are 32, 38 and 40 slotted models. There are six models in the same energy efficiency class (IE3) as RFIM. Only 34 slotted model is in a lower efficiency class (IE2).

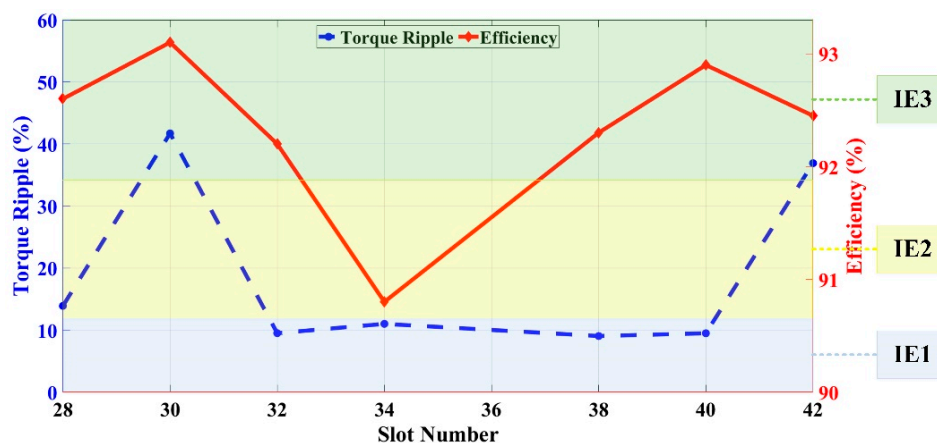


Figure 5. Efficiency and torque results of AFIM with different slot numbers.

As a result of the analyses made according to different rotor slot numbers, although it does not have the highest efficiency, it can be said that the 40 slotted model, which is in the same energy efficiency class and has little difference between its efficiency, is the best model among them since the torque ripple is much less.

3.4. Results of AFIM with Skewed Rotor

In the analysis of the rotor with 28 slot non-skew model, torque ripple 13.9%, efficiency 92.6% are obtained. The efficiency class of this model is in IE3 class. As the first analysis, skew angles are given to 28-slot AFIM. Accordingly, the skew angles in analyses are 10°, 12.86°, 15° and 20°. Torque ripple and efficiency results of the analyses are presented in Figure 6. Modeling of 25.72° skew is not feasible due to the overlay occurring between stator and rotor. In Figure 6, it is observed that there is no increase in efficiency when the rotor is skewed. However, when the models with skewed according to the number of stator slots are examined, it is seen that the efficiency decreases as the skew angle increases. On the other hand, when the skew is given according to the number of rotor slots, the efficiency keeps the same value.

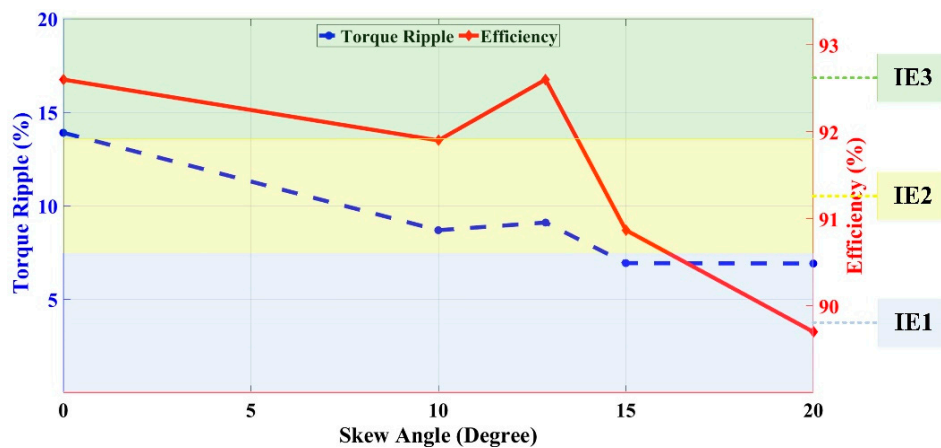


Figure 6. Efficiency and torque results of AFIM with 28 slots.

As a result of the non-skew model analyses, 30-slot AFIM model has the highest torque ripple value and the best efficiency. In the second analysis, this model is skewed. In addition to the non-skew model; in Figure 7 the torque ripple and the efficiency results of 10°, 12°, 15° and 20° skewed AFIM models are presented. In Figure 7, the torque ripple has decreased as the skew angle degree increases in analyses made only considering the number of stator slots. When analyses made according to the number of rotor slots are compared among themselves, it is seen that as the skew angle increases, the torque ripple decreases. In Figure 7, an increment in efficiency was not observed when the rotor is skewed. However, according to the skewed models, efficiency is increasing with the increment in the skew angle.

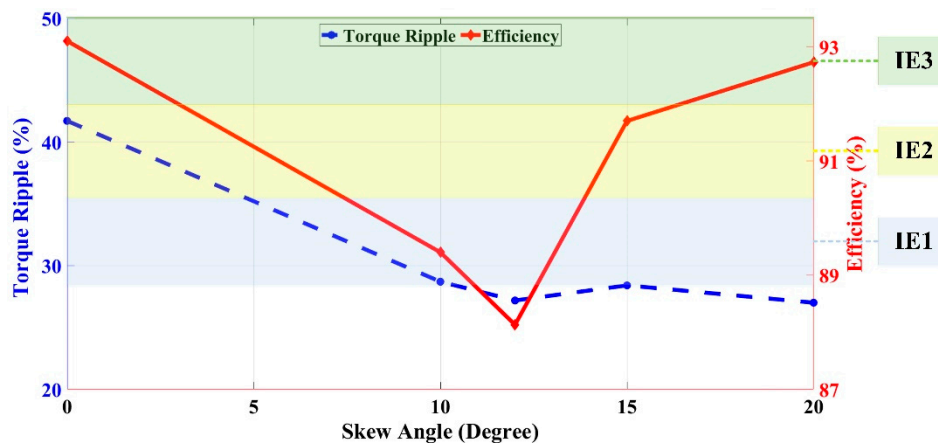


Figure 7. Efficiency and torque results of AFIM with 30 slots.

Considering the number of stators and rotor slots, the third analyses are done to 32-slot AFIM model with the skew angle of 10° , 11.25° , 15° , 20° and 22.5° . The non-skewed 32-slot AFIM model's torque ripple is 9.5% and the efficiency is 92.2%, which is in the IE3 class. Torque ripple and efficiency results of the analyses are shown in Figure 8. A comparison of the non-skew and 10° skew models shows that 10° skewed model has less torque ripple. On the other hand, a comparison of only skewed models shows that the torque ripple is lowest at 10° and highest at 15° . Comparing the 32-slot skewed models and the non-skew model, it is seen that the torque ripple decreases when the skew angle is 10° .

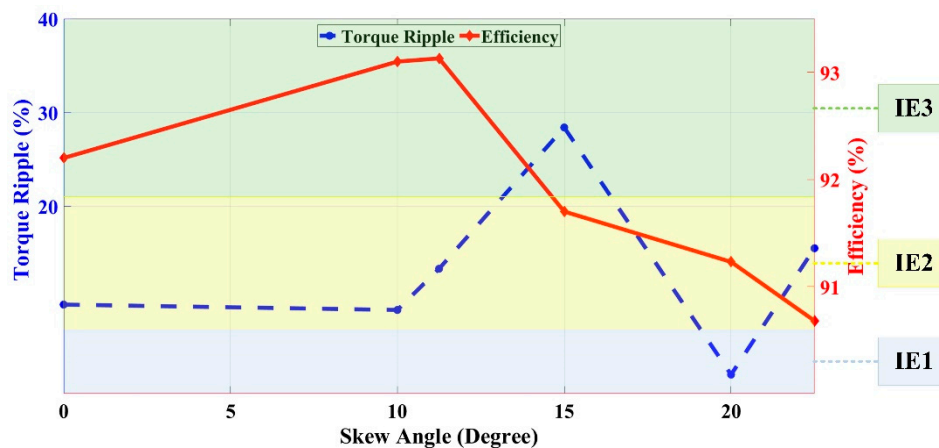


Figure 8. Efficiency and torque results of AFIM with 32 slots.

In addition, efficiency increases and the efficiency class increases from IE2 to IE3. Only from skewed models according to the number of stator slots, the efficiency decreases while the skew angle increases. On the other hand, according to the skewed models skewed with rotor slots number, the torque ripple increases and the efficiency decreases while the skew angle increases.

The fourth analysis is performed to 34-slot AFIM and the skew angles are calculated as 10° , 10.58° , 15° , 20° and 21.17° . In the 34-slot non-skewed model, the torque ripple is 11%, the efficiency is 90.8%, while the efficiency class is in the IE2 class. Torque ripple and efficiency results of the 32-slot AFIM analyses are shown in Figure 9. It is observed that the torque ripple does not fluctuate very much. Accordingly, it can be seen that the 15° skewed model is the most efficient model.

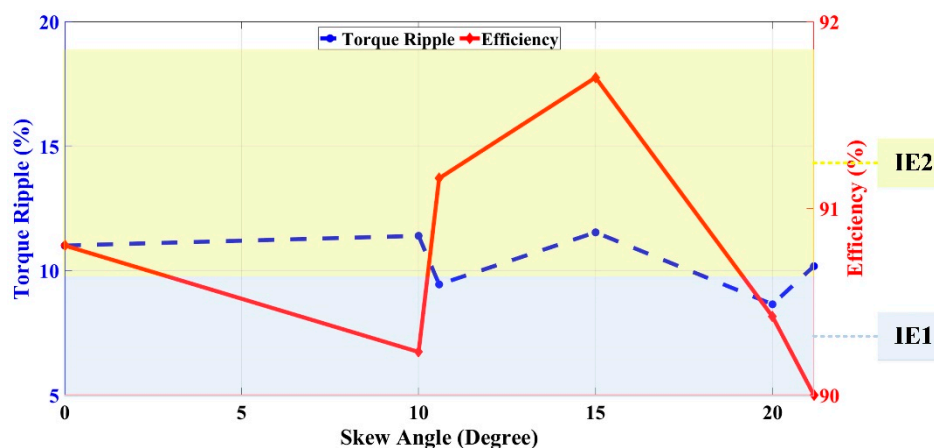


Figure 9. Efficiency and torque results of AFIM with 34 slots.

In the 5th analysis step, the 38-slot AFIM, which has the least torque ripple, is analyzed by considering the stator and rotor slots numbers. Accordingly, skew angles are determined as 9.47° , 10° , 15° , 18.95° and 20° . When the skewed analysis results are compared to the non-skewed model,

the analysis with the lowest torque ripple is obtained when the skew angle is 9.47. Torque ripple and efficiency results of the 38-slot AFIM analyses are shown in Figure 10.

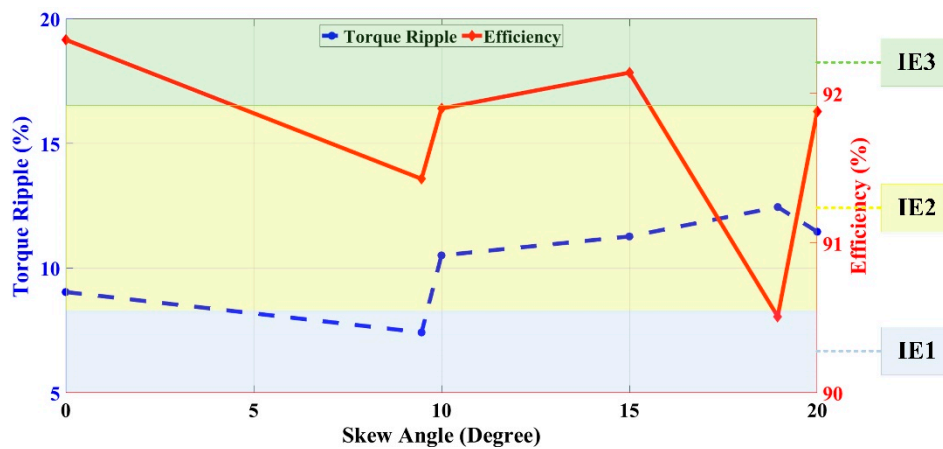


Figure 10. Efficiency and torque results of AFIM with 38 slots.

When the results of the skewed models of the 38-slot AFIM model according to the number of stator and rotor slots are examined, we do not see a positive effect on efficiency. Although the results are close to each other, the non-skewed model gives better results than skewed models.

In the sixth analysis step, the skew applied to the rotor of the 40-slot AFIM, which has the second best efficiency among non-skewed models. This model is also in IE3 energy efficiency class and the only model with low torque fluctuation. Skew angles for this model are calculated as 9° , 10° , 15° , 18° and 20° . Figure 11 shows the torque and efficiency results of the non-skewed and skewed models. In Figure 11, the 18° skewed model has the best torque ripple percentage. It can be seen that giving a skew to the rotor of 40-slot AFIM affects the efficiency negatively. However, the non-skewed, 9° , 10° , 15° and 18° skewed models are in IE3 energy efficiency class, other 10° and 20° skewed models are in IE2 energy efficiency class.

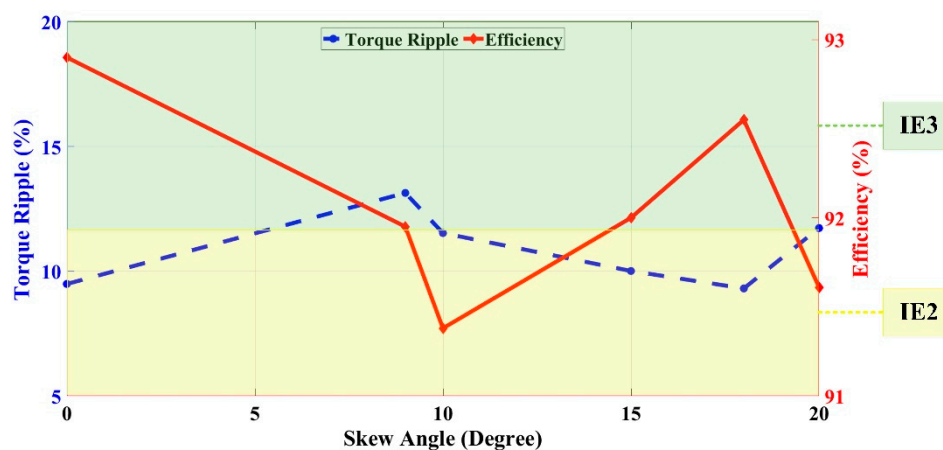


Figure 11. Efficiency and torque results of AFIM with 40 slots.

The last step of analyses among skewed models is done to 42-slot AFIM, which is another model with high torque ripple. Analyses results of non-skewed and skewed models of 42-slot AFIM are shown in Figure 12. The non-skewed model of 42-slot AFIM is in IE3 energy efficiency class. According to the analyses results, it is observed that there is a different situation between the efficiencies that are not encountered in the other slot numbers. Efficiency decreased in models with 10° and 20° skewed, whereas efficiency in skew angle 8.57° and 15° is significantly increased. In fact, it has been observed

that three of these models are in the IE4 energy efficiency class. These are the highest efficient models achieved among analyses.

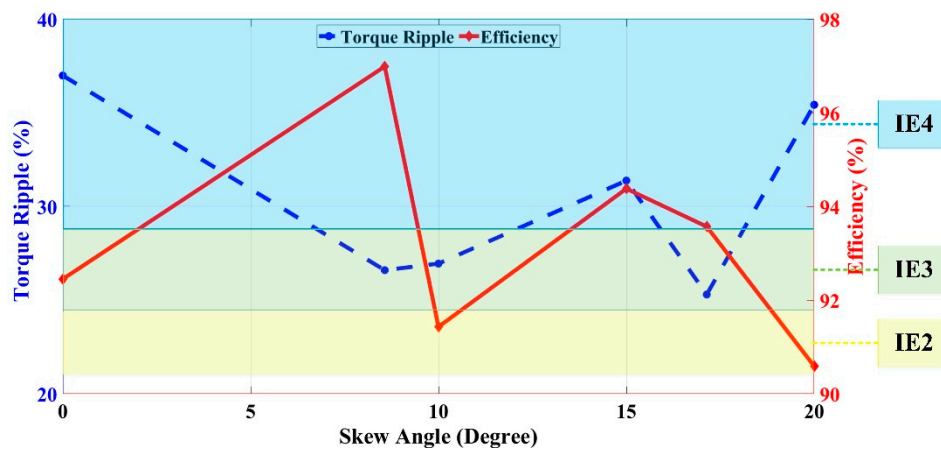


Figure 12. Efficiency and torque results of AFIM with 42 slots.

As a result of all analyses carried out, giving skews to the rotor of the motor affects the efficiency differently, and the torque ripple in different rotor slot numbers of AFIMs. In some AFIMs, skewing has a positive effect in terms of torque ripple and decreases the torque ripple, while in others it is observed that the torque ripple increases. In the same way, it has different effects in terms of efficiency. For example, the 8.57° , 15° and 17.14° skewed 42-slot AFIMs are given results in IE4 energy efficiency class. Also, the torque ripple of the same model decreases by 28% to 26.6%. Therefore, the best configuration among 42-slot models is obtained as 8.57° skew angle.

However, in the analyses performed both in terms of torque ripple and efficiency, the most optimum condition result is achieved in the design with a 10° skew given to the 32-slot AFIM. The torque ripple of this model is 8.93%, the efficiency is 93.1% and efficiency class of this motor is IE3. In the next section, the effect of the material on efficiency and torque ripple by using SMC material is examined.

3.5. Results of AFIM with SMC Material

In this section, the effect of the SMC material on efficiency and torque is examined. By this purpose, three analyses are done with using SMC material for stator, rotor and both of them. Somaloy 700-3P is selected as a SMC material with a density 7.57 g/cm^3 [42].

According to the analyses results, by changing the material, the efficiencies stayed in the same efficiency class as IE3. However, only SMC stator has the best efficiency value, both SMC stator&rotor has the best torque value. Compared to the non-skewed based model to both SMC stator&rotor used model over 11% of reduction is observed in torque ripple. Additionally, changing the material has a positive impact on the efficiency. Figure 13 shows the efficiency and torque results of SMC used AFIM by different parts.

In the X-axis of Figure 13, skew status and material of AFIM are defined as follows:

- Rotor is not skewed and both stator and rotor material are steel,
- Rotor is skewed and both stator and rotor material are steel,
- Rotor is skewed and stator material is SMC and rotor material is steel,
- Rotor is skewed and stator material is steel and rotor material is SMC,
- Rotor is skewed and both stator and rotor material are SMC.

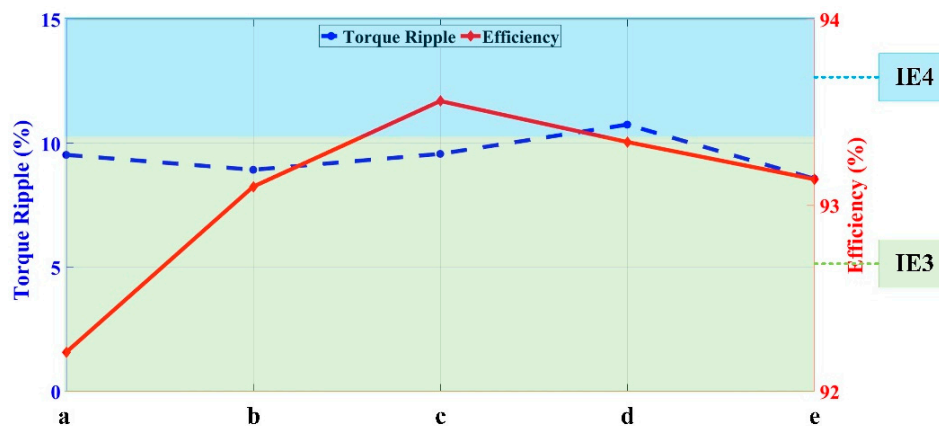


Figure 13. Efficiency and torque results of SMC used AFIM.

4. Conclusions

Since the aim in this study is to achieve an AFIM in the same energy efficiency class as RFIM, the efficiency of AFIMs with torque ripples are investigated. In this study, transient analyses are carried out and torque values are calculated with the help of ANSYS Maxwell program. Efficiency values of analysis results according to seven different slot numbers from 28 to 42 are presented. In addition to the efficiency values, the percentage torque ripples and energy efficiency class are also examined. To reduce the torque ripple values, rotor is skewed according to stator and rotor slot numbers. It was seen that the effects of skewing on efficiency and torque ripple are variable. Also, it was observed that to choose the skewing angle degrees, not only with stator slot number, but also rotor slot number could affect positive the performance of AFIMs. Using a SMC material on different parts of AFIM had a positive impact on performance analysis of a model, as reducing the torque ripple over 11% while the models are in premium efficiency class. For further studies, different materials could be used for various applications.

Author Contributions: F.K.A., I.S., Y.O. work on conceptualization, methodology, software, validation, formal analysis, writing—original draft preparation, writing—review and editing. All authors have read and agreed to the published version of the manuscript.

Funding: This research received no external funding.

Acknowledgments: The authors declare no acknowledgements.

Conflicts of Interest: The authors declare no conflict of interest.

References

- De Almeida, A.T.; Ferreira, F.J.T.E.; Fong, J.A.C. Standards for Efficiency of Electric Motors. *IEEE Ind. Appl. Mag.* **2010**, *17*, 12–19. [CrossRef]
- Ferreira, F.J.T.E.; Leprettre, B.; De Almeida, A.T. Comparison of Protection Requirements in IE2-, IE3-, and IE4-Class Motors. *IEEE Trans. Ind. Appl.* **2016**, *52*, 3603–3610. [CrossRef]
- Elvira-Ortiz, D.A.; Morinigo-Sotelo, D.; Zorita-Lamadrid, A.L.; Osornio-Rios, R.A.; Romero-Troncoso, R.d.J. Fundamental frequency suppression for the detection of broken bar in induction motors at low slip and frequency. *Appl. Sci.* **2020**, *10*, 4160. [CrossRef]
- Pietrowski, W.; Górný, K. Analysis of Torque Ripples of an Induction Motor Taking into Account a Inter-Turn Short-Circuit in a Stator Winding. *Energies* **2020**, *13*, 3626. [CrossRef]
- Esen, G.K.; Ozdemir, E. A New Field Test Method for Determining Energy Efficiency of Induction Motor. *IEEE Trans. Instrum. Meas.* **2017**, *66*, 3170–3179. [CrossRef]
- Parviainen, A. *Design of Axial-Flux Permanent-Magnet Low-Speed Machines and Performance Comparison between Radial-Flux and Axial-Flux Machines*; Lappeenranta University of Technology: Lappeenranta, Finland, 2005; ISBN 9522140295. Available online: <https://lutpub.lut.fi/bitstream/handle/10024/31185/TMP.objres.74.pdf?sequence=1> (accessed on 22 September 2020).

7. Boglietti, A.; Cavagnino, A.; Vaschetto, S. Induction motor EU standards for efficiency evaluation: The scenario after IEC 60034-2-1. In Proceedings of the IECON 2011—37th Annual Conference of the IEEE Industrial Electronics Society, Melbourne, VIC, Australia, 7–10 November 2011; pp. 2786–2791.
8. IEC-Governments & International Organizations, Examples by Industry Sector: Electric Motors-Measuring Efficiency. Available online: https://www.iec.ch/perspectives/government/sectors/electric_motors.htm (accessed on 18 March 2020).
9. Electric Motors | European Commission. Available online: https://ec.europa.eu/info/energy-climate-change-environment/standards-tools-and-labels/products-labelling-rules-and-requirements/energy-label-and-ecodesign/energy-efficient-products/electric-motors_en (accessed on 18 March 2020).
10. De Almeida, A.T.; Ferreira, F.J.T.E.; Baoming, G. Beyond induction motors—Technology trends to move up efficiency. *IEEE Trans. Ind. Appl.* **2014**, *50*, 2103–2114. [CrossRef]
11. Ferreira, F.J.T.E.; Baoming, G.; De Almeida, A.T. Reliability and operation of high-efficiency induction motors. In Proceedings of the 2015 IEEE/IAS 51st Industrial and Commercial Power Systems Technical Conference, I and CPS 2015, Calgary, AB, Canada, 5–8 May 2015; Institute of Electrical and Electronics Engineers Inc.: New York, NY, USA, 2015.
12. The Impact of New IE3 Requirements on Motors and Controls. Available online: <https://www.totallyintegratedautomation.com/2017/11/impact-new-ie3-requirements-motors-controls/> (accessed on 18 March 2020).
13. Valtonen, M.; Parviainen, A.; Pyrhönen, J. Electromagnetic field analysis of 3D structure of axial-flux solid-rotor induction motor. In Proceedings of the International Symposium on Power Electronics, Electrical Drives, Automation and Motion, Taormina, Italy, 23–26 May 2006; SPEEDAM 2006. Volume 2006, pp. 174–178.
14. Evans, P.D.; Eastham, J.F. Disc-geometry homopolar synchronous machine. *IEE Proc. B Electr. Power Appl.* **1980**, *127*, 299–307. [CrossRef]
15. Valtonen, M.; Parviainen, A.; Pyrhönen, J. The effects of the number of rotor slots on the performance characteristics of axial-flux aluminium-cage solid-rotor core induction motor. In Proceedings of the IEEE International Electric Machines & Drives Conference, Antalya, Turkey, 3–5 May 2007; Volume 1, pp. 668–672.
16. Dianati, B.; Kahourzade, S.; Mahmoudi, A. Analytical design of axial-flux induction motors. In Proceedings of the 2019 IEEE Vehicle Power and Propulsion Conference, VPPC 2019—Proceedings, Hanoi, Vietnam, 14–17 October 2019; Institute of Electrical and Electronics Engineers Inc.: New York, NY, USA, 2019.
17. Rodger, D.; Coles, P.C.; Allen, N.; Lai, H.C.; Leonard, P.J.; Roberts, P. 3D finite element model of a disc induction machine. In Proceedings of the IEE Conference Publication, Cambridge, UK, 1–3 September 1997; pp. 148–149.
18. Valtonen, M.; Parviainen, A.; Pyrhönen, J. Inverter switching frequency effects on the rotor losses of an axial-flux solid-rotor core induction motor. In Proceedings of the POWERENG 2007—International Conference on Power Engineering—Energy and Electrical Drives Proceedings, Setubal, Portugal, 12–14 April 2007.
19. Dianati, B.; Kahourzade, S.; Mahmoudi, A. Optimization of Axial-Flux Induction Motors for the Application of Electric Vehicles Considering Driving Cycles. *IEEE Trans. Energy Convers.* **2020**, *35*, 1522–1533. [CrossRef]
20. Mei, J.; Lee, C.H.T.; Kirtley, J.L. Design of axial flux induction motor with reduced back iron for electric vehicles. *IEEE Trans. Veh. Technol.* **2020**, *69*, 293–301. [CrossRef]
21. Benoudjit, A.; Guettafi, A.; Nait Saïd, N. Axial flux induction motor for on-wheel drive propulsion system. *Electr. Mach. Power Syst.* **2000**, *28*, 1107–1125. [CrossRef]
22. Álvarez, A.; Suárez, P.; Cáceres, D.; Cordero, E.; Ceballos, J.M.; Pérez, B. Disk-shaped superconducting rotor under a rotating magnetic field: Speed dependence. *IEEE Trans. Appl. Supercond.* **2005**, *15*, 2174–2177. [CrossRef]
23. Kubzdela, S.; Weglinski, B. Magnetodielectrics in Induction Motors with Disk Rotor. *IEEE Trans. Magn.* **1987**, *24*, 635–638. [CrossRef]
24. Beleiu, H.G.; Maier, V.; Pavel, S.G.; Birou, I.; Pica, C.S.; Darab, P.C. Harmonics consequences on drive systems with induction motor. *Appl. Sci.* **2020**, *10*, 1528. [CrossRef]
25. Carbonieri, M.; Bianchi, N. Induction motor rotor losses analysis methods using finite element. In Proceedings of the 2020 IEEE International Conference on Industrial Technology (ICIT), Buenos Aires, Argentina, 26–28 February 2020; pp. 187–192.

26. Nobahari, A.; Darabi, A.; Hassannia, A. Various skewing arrangements and relative position of dual rotor of an axial flux induction motor, modelling and performance evaluation. *IET Electr. Power Appl.* **2018**, *12*, 575–580. [[CrossRef](#)]
27. Le Besnerais, J.; Lanfranchi, V.; Hecquet, M.; Romary, R.; Brochet, P. Optimal slot opening width for magnetic noise reduction in induction motors. *IEEE Trans. Magn.* **2009**, *45*, 3131–3136. [[CrossRef](#)]
28. Hecker, Q.; Igelspacher, J.; Herzog, H.G. Parameter identification of an axial-flux induction machine by winding functions. In Proceedings of the 19th International Conference on Electrical Machines- ICEM 2010, Rome, Italy, 6–8 September 2010.
29. Chan, C.C. Axial-field electrical machines—Design and applications. *IEEE Trans. Energy Convers.* **1987**. [[CrossRef](#)]
30. Nasiri-Gheidari, Z.; Lesani, H. New design solution for static eccentricity in single stator-single rotor axial flux induction motors. *IET Electr. Power Appl.* **2013**, *7*, 523–534. [[CrossRef](#)]
31. Nobahari, A.; Darabi, A.; Hassannia, A. Axial flux induction motor, design and evaluation of steady state modeling using equivalent circuit. In Proceedings of the 8th Power Electronics, Drive Systems and Technologies Conference, PEDSTC 2017, Mashhad, Iran, 14–16 February 2017.
32. Patterson, D.J.; Colton, J.L.; Mularcik, B.; Kennedy, B.J.; Camilleri, S.; Rohoza, R. A comparison of radial and axial flux structures in electrical machines. In Proceedings of the 2009 IEEE International Electric Machines and Drives Conference, IEMDC '09, Miami, FL, USA, 3–6 May 2009; pp. 1029–1035.
33. Mirzaei, M.; Mirsalim, M.; Abdollahi, S.E. Analytical modeling of axial air gap solid rotor induction machines using a quasi-three-dimensional method. *IEEE Trans. Magn.* **2007**, *43*, 3237–3242. [[CrossRef](#)]
34. Nasiri-Gheidari, Z.; Lesani, H. A survey on axial flux induction motors. *Prz. Elektrotechniczny* **2012**, *2*, 300–305.
35. Babu, V.R.; Soni, M.P. Modelling of Twin Rotor Axial Flux Induction Machine and its Application as Differential in Electrical Vehicles. *IJIREEICE* **2017**, *5*, 118–127. [[CrossRef](#)]
36. Egea, A. Overview of Axial Flux Machines. *Electr. Energy Mag.* **2013**, *4*, 2–13.
37. Varga, J.S. Magnetic and Dimensional Properties of Axial Induction Motors. *IEEE Trans. Energy Convers.* **1986**, *EC-1*, 137–144. [[CrossRef](#)]
38. Pyrhönen, J.; Jokinen, T.; Hrabovcová, V. *Design of Rotating Electrical Machines*; John Wiley & Sons: West Sussex, UK, 2008; ISBN 9780470695166.
39. IEEE. *IEEE Standard Test Procedure for Polyphase Induction Motors and Generators*; IEEE Std 112-2017 (Revision of IEEE Std 112-2004); IEEE: Piscataway, NJ, USA, 2018; pp. 1–115. [[CrossRef](#)]
40. Yamazaki, K.; Haruishi, Y. Stray load loss analysis of induction motor comparison of measurement due to IEEE standard 112 and direct calculation by finite element method. In Proceedings of the IEEE International Electric Machines and Drives Conference, IEMDC'03, Madison, WI, USA, 1–4 June 2003; Volume 1, pp. 285–290.
41. Levi, E.; Lamine, A.; Cavagnino, A. Impact of stray load losses on vector control accuracy in current-fed induction motor drives. *IEEE Trans. Energy Convers.* **2006**, *21*, 442–450. [[CrossRef](#)]
42. Somaloy® Quick Guide. Available online: https://www.hoganas.com/globalassets/download-media/sharepoint/brochures-and-datasheets---all-documents/somaloy-quick-guide_july_2015_1122hog.pdf (accessed on 20 September 2020).

